Chinese J. Chem. Eng., **10** (5) 522 – 528 (2002)

Computational Fluid-dynamics of Liquid Phase Flow on Distillation Column Trays*

LIU Chunjiang(刘春江) and **YUAN Xigang(袁希钢)**
Distillation Laboratory of State Key Laboratories of Chemical Engineering, Tianjin University, Tianjin 300072, China

Abstract A computational fluid-dynamics model is presented for predicting the two-phase two-dimensional liquid phase flow on a distillation column tray based on the modification of Navier-Stokes Equation by considering both the resistance and the enhanced turbulence created by the uprising vapor. Experimental measurement of the local liquid phase velocity on an air-water simulator of 1.2 m in diameter by using the hot film anemometer is briefly described. Two of the conventional fluid-dynamic constants are readjusted for the case of liquid flow on a tray by fitting the experimental data. The predicted local liquid phase velocity and direction of flow by the present model are confirmed satisfactorily by the authors' experimental measurements and by the data from literature. By the aid of the present model, the concentration field on the tray can be computed for the evaluation of the enhancement of liquid phase concentration across a tray. The advantages of applying computational fluid-dynamics to tray column design are discussed.

Keywords computational fluid-dynamics, gas-liquid two-phase flow, distillation column tray, fluid mechanics, concentration profile

1 INTRODUCTION

It is well known that the liquid flow pattern, or velocity distribution, is an important factor in column tray design, yet its evaluation has long been relied mainly on designer's experience or experiment, implicitly in the estimation of tray efficiency. The theoretical approach of such problem is possible upon the light of computational fluid-dynamics as many software for calculating the flow distribution are available in the market. The basic flow model used in the commercial software may not be suitable to the condition of a column tray, and therefore the computed result deviates in some extent from the experimental measurement and fails in the cases of having high percentage of liquid circulation. Since the liquid phase velocity distribution and, particularly, the liquid circulation on a tray may reduce seriously the tray efficiency and should be prevented early in column design, the investigation of more accurate modeling of flow pattern is therefore still in need.

The difficulty of theoretical prediction of liquid flow pattern on a column tray comes from the complicated fact that it is an aerated liquid flowing through a curved convergent-divergent open channel with structural resistance and subject simultaneously to the action of the cross current uprising vapor. Based on the two dimensional liquid flow with some simplifying assumptions, Yoshida[1] presented a solution by using the method of stream function, but his result has not been confirmed by experiment. Yu *et al.*[2,3] employed the fundamental equations of Navier-Stokes and Reynolds together with the k-ε equations of turbulence, and obtained the solution numerically. Their predictions of liquid velocity distribution on a tray were satisfactorily checked by the results taken on experimental sieve trays of 1.2 and 2.4 meters in diameter[3,4], involving the operation at high percentage of liquid circulation. They formulated two different kinds of liquid flow model, *i.e.* single-fluid (liquid) model[2] and two-fluid (liquid and vapor) model[3], with considering the resistance created by the cross-current vapor. The two-fluid model gives slightly better result than the single-fluid model at the expense of much more complicated computation. Krishna *et al.*[5] presented a three dimensional model and solved by using commercial software CFX for simulating the transient liquid flow on a 0.2×0.39 meters rectangular sieve tray. In the present study, a modified single-fluid model is presented for its simple form with sufficient accuracy and the convenience of applying it to the computation of concentration distribution on a tray in order to make the evaluation of tray efficiency reliable and on a sound basis.

2 EXPERIMENTAL EVIDENCE

Our experimental work was performed in a water-air sieve tray simulator of 1.2 m in diameter as shown schematically in Fig. 1. The tray is single-pass with sieve holes diameter of 4.6 mm and having 4.6% opening of tray area. The length of both inlet and outlet

Received 2002-04-08, accepted 2002-06-08.
* Supported by Visiting Scholar Foundation of Key Lab in Tianjin University.
** To whom correspondence should be addressed. E-mail: cjliu@tju.edu.cn

weirs is 0.79 m, and the height of outlet weir is either 25 mm or 50 mm. All the experimental operations were adjusted to the condition of dominated bubbling over the tray at the water rate up to $0.03\,m^3\cdot m^{-1}\cdot s^{-1}$ and the superficial air velocity up to $1.3\,m\cdot s^{-1}$. The local velocity of liquid was measured by using hot film anemometer supplied by TSI company equipped with X-type probe, intellectual velocity analyzer and A/D converter. The experimental data were recorded and processed by a computer. Although such instrument has been used for the measurement of single and two-phase concurrent flow, the application to the case of air-water crosscurrent flow is successful only by the aid of improved technique. In the present work, the two-dimensional liquid velocities, in respect to the directions of parallel and perpendicular to the weir, at various locations and liquid depths were measured.

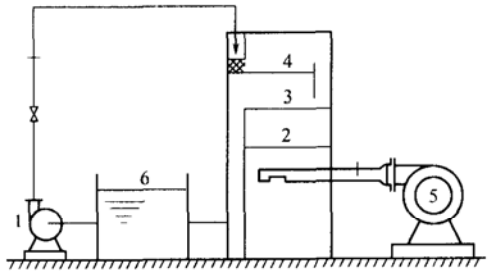

Figure 1 Schematic diagram of experimental set-up
1—circulating pump; 2, 3—distribution plate; 4—test tray (1.2 m in diameter); 5—blower; 6—water tank

Experimental measurement indicated that no appreciable liquid velocity gradient along the liquid depth was found if the measuring probe was placed about 10 mm above the bubbling tray floor. Exception was found only at the regions near the inlet and outlet weirs. A typical measuring result at the main flow region is given in Table 1. The disappearance of velocity gradient along the liquid depth may be due to the fact that the uprising bubbles from the sieve holes destroy the boundary layer of liquid flow on the tray floor and thus prevent the formation of the velocity gradient. On the other hand, the agitation effect of the air bubbles on the water also tends to reduce the gradient. Such experimental evidence allows us to make the assumption in the following modeling that the liquid flow on a tray is substantially two-dimensional except around the small regions near the inlet and outlet weirs.

Table 1 Experimental measurement of local liquid velocity u along liquid depth h_l
($L = 0.079\,m^3\cdot m^{-1}\cdot s^{-1}$, $u_w = 0.645\,m\cdot s^{-1}$)

h_l, mm	u, $cm\cdot s^{-1}$	$\left\|\frac{u-\overline{u}}{\overline{u}}\right\|$, %
10	25.381	0.29
15	26.205	3.55
20	24.872	1.72
25	25.998	2.73
30	25.298	0.04
35	24.207	4.35
40	25.089	0.86

3 TWO-DIMENSIONAL PSEUDO SINGLE FLUID MODEL

In the present model, the "fluid" flowing across the tray includes both liquid and holdup bubbles, and behaves as a "single fluid". The action of uprising vapor (air) is considered as a body force acting on the fluid. In applying the classical equations of Navier-Stokes and Reynolds, the following two factors should be considered:

(1) *The resistance to the fluid flow created by the uprising vapor*

The resistance created by the uprising (penetrating) vapor to the fluid flow is considered to be equivalent to a body force acting vertically and uniformly on the horizontally flowing fluid. This body force, f, may be resolved into f_x and f_y in x and y directions. Then we have[2,3]

$$f_x = \frac{C_r \rho_b w u}{h} \tag{1}$$

$$f_y = \frac{C_r \rho_b w v}{h} \tag{2}$$

where C_r is the coefficient of momentum transfer, ranging from 0 to 1, depending on the transfer efficiency. From our experiment in a small air-water simulator, the coefficient C_r can be taken equal to 0.8.

(2) *The increase of fluid turbulent energy due to bubbling action and frictional resistance*

The increase of fluid turbulent energy as a result of bubbling action, or agitation, by the penetrating bubbles may be understood as follows. For stationary liquid, the time average velocity of the liquid in all directions is equal to zero. If an uprising bubble penetrates through the liquid, the time average velocity of the liquid in all directions is still equal to zero, while its fluctuation velocity is not. It means that certain amount of turbulent energy of the liquid is being produced by the action of bubbling. As the amount of turbulent energy produced by both bubbling action and frictional resistance on the tray are difficult to evaluate, we may represent it by a term G_p, the value of which will be given in the subsequent section.

3.1 The governing equations

In the present model, the method of k-ε equation is used for the closure of the basic equations. The control equations are as follows:

continuity equation

$$\frac{\partial \rho u}{\partial x} + \frac{\partial \rho v}{\partial y} = 0 \tag{3}$$

momentum equations

$$u\frac{\partial u}{\partial x}+v\frac{\partial u}{\partial y}=-\frac{1}{\rho}\frac{\partial p}{\partial x}+\frac{\partial}{\partial x}\left(\vartheta_e\frac{\partial u}{\partial x}\right)+\frac{\partial}{\partial y}\left(\vartheta_e\frac{\partial u}{\partial y}\right)+\frac{f_x}{\rho} \tag{4}$$

$$u\frac{\partial v}{\partial x}+v\frac{\partial v}{\partial y}=-\frac{1}{\rho}\frac{\partial p}{\partial y}+\frac{\partial}{\partial x}\left(\vartheta_e\frac{\partial v}{\partial x}\right)+\frac{\partial}{\partial y}\left(\vartheta_e\frac{\partial v}{\partial y}\right)+\frac{f_y}{\rho} \tag{5}$$

k equation

$$u\frac{\partial k}{\partial x}+v\frac{\partial k}{\partial y}=\frac{\partial}{\partial x}\left(\frac{\vartheta_e}{\sigma_k}\frac{\partial k}{\partial x}\right)+\frac{\partial}{\partial y}\left(\frac{\vartheta_e}{\sigma_k}\frac{\partial k}{\partial y}\right)+G_T+G_p-\varepsilon \tag{6}$$

ε equation

$$u\frac{\partial \varepsilon}{\partial x}+v\frac{\partial \varepsilon}{\partial y}=\frac{\partial}{\partial x}\left(\frac{\vartheta_e}{\sigma_\varepsilon}\frac{\partial \varepsilon}{\partial x}\right)+\frac{\partial}{\partial y}\left(\frac{\vartheta_e}{\sigma_\varepsilon}\frac{\partial \varepsilon}{\partial y}\right)+\left[C_1\left(G_T+G_p\right)-C_2\varepsilon\right]\frac{\varepsilon}{k} \tag{7}$$

where G_T, the generation of turbulent energy by the main fluid flow, is given by

$$G_T=\vartheta_t\left[2\left(\frac{\partial u}{\partial x}\right)^2+2\left(\frac{\partial v}{\partial y}^2\right)+\left(\frac{\partial u}{\partial y}+\frac{\partial v}{\partial x}\right)^2\right] \tag{8}$$

and G_p, the turbulent energy produced as a result of bubbling action and frictional resistance, is an unknown quantity which will be determined experimentally as shown in the later section.

The relationships between effective viscosity ϑ_e, turbulent viscosity ϑ_t and the fluid viscosity μ are given below

$$\vartheta_e=\vartheta_t+\frac{\mu}{\rho} \tag{9}$$

$$\vartheta_t=C_\mu\frac{k^2}{\varepsilon} \tag{10}$$

It should be noted that all the fluid properties, such as fluid viscosity μ and density ρ refering to the liquid and bubble mixture, are calculated as follows

$$\mu=\alpha_l\mu_l+\alpha_b\mu_b$$

$$\rho=\alpha_l\rho_l+\alpha_b\rho_b$$

where the subscript l and b denote the liquid and the bubble phase correspondingly. All other fluid parameters, such as velocity u, v, the effective viscosity ϑ_e and turbulent viscosity ϑ_t are considered to be unique for the fluid, and the proportional rule cannot be applied.

3.2 The boundary conditions

For the inlet condition, uniform fluid flow in x direction is assumed

$$u_{in}=\frac{L}{h}\quad\text{and}\quad u_{in}=0 \tag{11}$$

where the height of equivalent clear liquid h is given by our experimental correlation as follows

$$h=8.04+0.308L+2.523h_w^{0.5}-3.612\times10^{-3}F_0^2 \tag{12}$$

The inlet k and ε were taken from an empirical correlation for the case of expended flow with vortex[6], *viz*

$$k_{in}=0.003u_{in}^2 \tag{13}$$

$$\varepsilon_{in}=6\frac{k_{in}^{\frac{3}{2}}}{l_w} \tag{14}$$

For the centerline boundary, symmetrical velocity field is assumed and given by

$$\frac{\partial u}{\partial y}=\frac{\partial k}{\partial y}=\frac{\partial \varepsilon}{\partial y}=0 \tag{15}$$

$$v=0 \tag{16}$$

For the outlet boundary, the flow is considered being fully developed, and the following conditions are applied

$$\frac{\partial u}{\partial x}=\frac{\partial v}{\partial x}=\frac{\partial k}{\partial x}=\frac{\partial \varepsilon}{\partial x}=0 \tag{17}$$

For the wall boundary, the condition as described by Nallasamy[6] is adopted. Since the wall boundary of the column tray is of circular shape, we assume that the direction of fluid flow along the wall is always tangential, and the following modified conditions are obtained

$$u=U\frac{Y}{R} \tag{18}$$

$$v=U\frac{X}{R} \tag{19}$$

$$K=\frac{u_\tau^2}{\sqrt{C_\mu}} \tag{20}$$

$$\varepsilon=\frac{u_\tau^3}{\kappa r_p} \tag{21}$$

where

$$U=\frac{u_\tau}{\kappa}\ln\left(r^+E\right) \tag{22}$$

$$u_\tau=\sqrt{\frac{\tau_w}{\rho}} \tag{23}$$

$$\tau_w=\frac{\kappa^*\rho U_p k^{\frac{1}{2}}}{\ln\left(E^*r_p k^{\frac{1}{2}}/\vartheta_e\right)} \tag{24}$$

$$r^+=\frac{r_p u_\tau}{\upsilon} \tag{25}$$

$$r_p=R-\sqrt{X^2+Y^2} \tag{26}$$

$$\kappa^* = \kappa C_\mu^{1/4} \tag{27}$$

$$E^* = E C_\mu^{1/4} \tag{28}$$

In the foregoing equations, U is the directional fluid velocity at a point near the wall with coordinates X and Y referring to the center of a tray as origin, R is the tray radius, E is the roughness parameter of the wall which can be taken to be 9, and κ, the Karman constant, is equal to 0.418.

3.3 The adjustment of fluid-dynamic constants

In our computation, the method of finite volume based on SIMPLE (Semi-implicit method for pressure link equation) algorithm was used, which has been described by Patankar[7].

As first approximation, the fluid-dynamic constants in the present model were taken from the experimental work of Launder[8] based on the tunnel flow, *i.e.*

$$C_\mu = 0.09,\ C_1 = 1.44,\ C_2 = 1.92,\ \sigma_k = 1.0,\ \sigma_\varepsilon = 1.3$$

In order to test the validity of these constants, the experiment of water flowing through a non-perforated tray simulator of 1.2 m in diameter, as described in previous section, was conducted. Under the condition of no air flow, the parameters G_p, f_x and f_y are equal to zero and the present model reduces to that of water flow only. Our experimental data together with that published by Porter *et al.*[4] on a simulator of 2.4 m in diameter are shown in Fig. 2, where the percentage of water circulation area on the tray is plotted against the rate of water flow. Whether or not to predict accurately the water circulation area on a tray is a critical criteria to the validity of a fluid-dynamic model for the extent of circulation area is one of the chief factors affecting the tray efficiency and should be considered seriously in tray design.

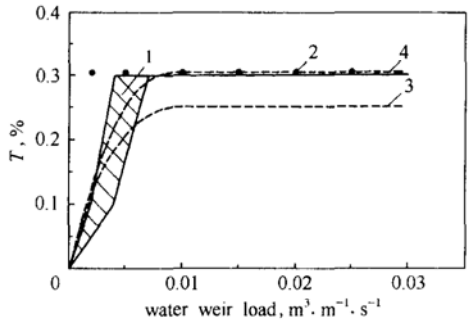

Figure 2 Adjustment of constants by experimental data on water flow across an non-perforated tray
1—boundary of experimental points by Porter *et al.*;
2—authors' experimental data;
3—model computation using constants by Launder *et al.*;
4—model computation using constants by the authors

As seen in Fig. 2, the computed result by using Launder's constants in present model can not fit the experimental data, and should be modified. After a number of trials, the constants C_1 and C_2 were found to be more sensitive than other constants. For the best fitting, the following values for C_1 and C_2 are recommended for using in the present model

$$C_1 = 1.48, \quad C_2 = 1.98$$

3.4 The determination of parameter G_p

With the adjusted constants C_1, C_2 and a series of assumed value of G_p , the computed results by present model for air-water flow were compared with our experimental data and that from Ref. [8]. It was found that the value of G_p is very sensitive in giving the percentage of circulation area as illustrated in Fig. 3. By finding the optimal values of G_p for the best matching of the circulation area in all the experimental runs, we found the following empirical relationship

$$G_\mathrm{p} = 1.28 \times 10^{-4} u_\mathrm{s} L^{-0.75} \tag{29}$$

The foregoing equation is in common with our observation that the G_p is increased either by increasing air velocity u_s or by decreasing the water rate L.

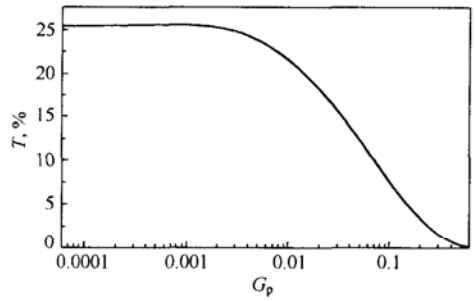

Figure 3 Effect of the parameter G_p on the percentage of circulation area T

4 EXPERIMENTAL VERIFICATION

Experimental work for verifying the velocity distribution predicted by the present model was carried out in the installation as described in Section 2. Since we assume that the velocity of water and holdup bubble is the same, the measurement of local water velocities at different locations on the tray by means of hot film anemometer can be used to check the accuracy of prediction by the present model. A typical velocity field is shown in Fig. 4, indicating the comparison between the experimental and computed results. The values in the parenthesis and the directional arrow with a small circle at the tail represent, respectively, the computed local velocity and flow direction by the present model. As can be seen, the model computation is satisfactorily confirmed by the experimental results. Also, the circulation area on the tray as shown in Fig. 4 is estimated to be around 12.6%, which is very close to

the model prediction of 12.4%. Similar confirmation is also obtained for a number of experimental measurements under different operating conditions on the simulated tray.

The experimental data from the literature suitable for checking the accuracy of the present model is the one by Porter *et al.*[4] in a 2.4 meters air-water simulator, the comparison is shown in Fig. 5 in which the model prediction is seen to be satisfactorily confirmed.

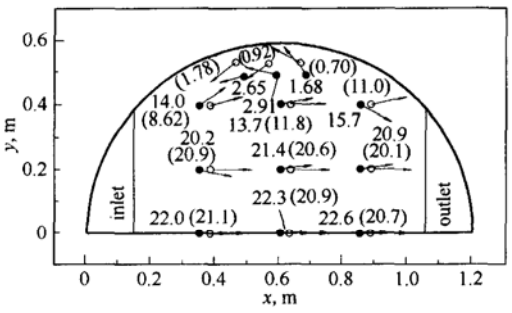

Figure 4 Comparison between model prediction and experimental data
($D = 1.2\,\mathrm{m}$, $L = 0.006\,\mathrm{m^3 \cdot m^{-1} \cdot s^{-1}}$, $w = 0.7\,\mathrm{m \cdot s^{-1}}$, $h_w = 25\,\mathrm{mm}$, $W/D = 0.645$)
●⟶ experimental result;
○⟶ computed result

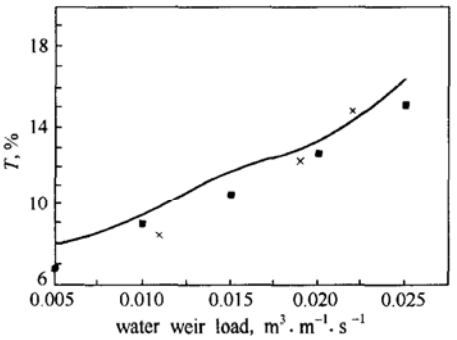

Figure 5 Comparison between model prediction and experimental data
($w = 1.25\,\mathrm{m \cdot s^{-1}}$, $h_w = 25\,\mathrm{mm}$)
—— model prediction;
■ experimental points by Porter *et al.*;
× experimental points by the authors

5 THE APPLICATION OF CFD TO THE EVALUATION OF TRAY EFFICIENCY

The successful application of computational fluid-dynamics (CFD) to the prediction of velocity field of a column tray may lead to the development of a method to evaluate the corresponding concentration field, from which the estimation of tray efficiency may be established on scientific and reliable basis. The two-dimensional mass diffusion equation of a component can be obtained by taking the material balance around a differential element consisting of the incoming and the exiting fluxes of mass, eddy diffusion and mass transferred from the passing vapor, and expressed as follows

$$u\frac{\partial c}{\partial x} + v\frac{\partial c}{\partial y} = D_e\frac{\partial^2 c}{\partial x^2} + D_e\frac{\partial^2 c}{\partial y^2} + J \tag{30}$$

$$J = k_l a\,(\dot{x} - \dot{x}^*) = k_g a\,(\dot{y}^* - \dot{y}) \tag{31}$$

where D_e is the effective diffusivity, which may be regarded as the sum of the molecular diffusivity and the turbulent (eddy) diffusivity by the theory of mixing length. Furthermore, by substituting, $c = \rho\dot{x}$ we have

$$u\frac{\partial \dot{x}}{\partial x} + v\frac{\partial \dot{x}}{\partial y} = D_e\frac{\partial^2 \dot{x}}{\partial x^2} + D_e\frac{\partial^2 \dot{x}}{\partial y^2} + \frac{k_l a}{\rho}(\dot{x} - \dot{x}^*) \tag{32}$$

The boundary conditions are similar to that of fluid flow including uniform incoming concentration *etc.* The foregoing equation may be solved simultaneously with the corresponding CFD equations to obtain the concentration field on the tray. The difficulty encountered in this problem may be on the estimation of D_e and mass transfer coefficient.

According to the rule of similarity, there exists a relationship between the effective viscosity in fluid-dynamics ϑ_e and the effective diffusivity D_e in mass transfer. From Prandtl's classical theory of mixing length, ϑ_e and D_e are of the same value. Previous work[9] indicated that these two parameters are in the same order of magnitude and the ratio of D_e/ϑ_e is approximately constant at 1.6. By taking the ϑ_e computed by the present CFD model, *i.e.* by solving Eqs. (3) to (7) and the D_e by the correlations of AIChE[10] and of Yu *et al.*[11] for the flow on a sieve tray, the ratios of D_e/ϑ_e are given in Table 2, ranging from 1.0 to 1.4. If the discrepancy between different models and experimental error are being considered, it is reasonable to take the average value of $D_e = 1.25\vartheta_e$ in our computation. Furthermore, our computation revealed that a slightly different ratio to be used does not change substantially the concentration profile on the tray.

To generalize the computational results of the concentration distribution on a tray, a parameter X, dimensionless concentration, is introduced and defined as follows

$$X = \frac{\dot{x} - \dot{x}^*}{\dot{x}_{in} - \dot{x}^*} \tag{33}$$

Note that, in foregoing equation, $X = 1$ and $X = 0$ represent respectively the initial and equilibrium conditions. Substituting Eq. (33) into Eq. (32), the mass transfer equation then becomes

$$u\frac{\partial X}{\partial x} + v\frac{\partial X}{\partial y} = D_e\frac{\partial^2 X}{\partial x^2} + D_e\frac{\partial^2 X}{\partial y^2} + \frac{k_l a}{\rho}X \tag{34}$$

Table 2 The ratio of effective viscosity ϑ_e and effective diffusive coefficient D_e on a sieve tray
($L = 0.00524\,m^3\cdot m^{-1}\cdot s^{-1}$, $h_w = 25\,mm$, $D = 2.44\,m$, $W/D = 0.6145$)

w, $m\cdot s^{-1}$	D_e		ϑ_e		
	AIChE correlation (A)	Yu *et al.* correlation (B)	Present model (C)	$\frac{(C)}{(A)}$	$\frac{(C)}{(B)}$
0.5	1.97×10^{-3}	1.40×10^{-3}	1.86×10^{-3}	1.4	1.3
1.0	2.80×10^{-3}	2.03×10^{-3}	2.45×10^{-3}	1.4	1.2
1.5	3.78×10^{-3}	2.78×10^{-3}	3.07×10^{-3}	1.2	1.1
2.0	4.90×10^{-3}	3.65×10^{-3}	3.67×10^{-3}	1.3	1.0

The foregoing equation can be solved simultaneously with the CFD equations to give a map of dimensionless concentration over a column tray under various operating conditions.

Since the range of concentration over a tray usually is not very wide, it is allowable to assume that the relationship $\dot{y} = m\dot{x}$ is held. The mass transfer equation may also be expressed alternatively in terms of mass transfer coefficient $k_g a$ as follows

$$u\frac{\partial X}{\partial x} + v\frac{\partial X}{\partial y} = D_e\frac{\partial^2 X}{\partial x^2} + D_e\frac{\partial^2 X}{\partial y^2} + \frac{k_g a}{m\rho}X \quad (35)$$

A typical concentration field on a column tray is shown schematically by drawing the smooth contours through the grids having practically the constant value of X as shown in Fig. 6. The reduction of concentration and the irregularity of having looped contours in the segmental region due to liquid circulation are clearly seen.

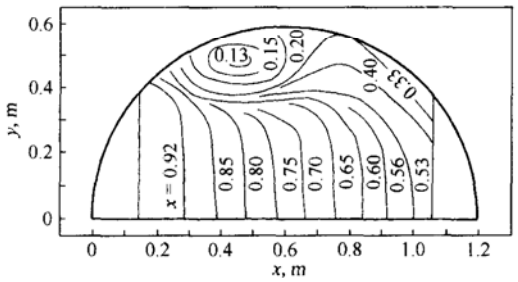

Figure 6 Dimensionless concentration profiles on a sieve tray
($D = 1.2\,m$, $L = 0.006\,m^3\cdot m^{-1}\cdot s^{-1}$; $w = 0.7\,m\cdot s^{-1}$; $h_w = 25\,mm$, $W/D = 0.645$)

The concentration enhancement across a tray, η, is defined as the ratio of the average liquid phase dimensionless concentration on the whole tray to that at the outlet weir. Thus $\eta = 1$ represents the condition of perfect mixing of liquid phase on a tray. For the case of partial mixing of liquid phase, η is greater than 1. Under the condition of no mixing, *i.e.* the plug flow, η reaches to the maximum. Obviously, η is a measure of the mixing characteristics on a tray or the relative tray efficiency, similar to the conventional expression E_{ML}/E_{OL}. The value of η can be computed by summing up the value of X in each grid obtained from the numerical computation as follows

$$\eta = \frac{\frac{1}{n_T}\sum_{n} X}{\frac{1}{n_w}\sum_{n_w} x_w} \quad (36)$$

The computed value of η is equal to 1.38 for the tray as shown in Fig. 6 under the operating conditions concerned. It demonstrates that the computation of tray efficiency is possible by the aid of CFD and mass transfer coefficient. The tray design based on such foundation is obviously superior to that based on experience or rough estimation, especially for the case of scaling up a column to large diameter.

It is interested to note the similarity between velocity and concentration fields, *i.e.* Figs. 4 and 6, where the main flow region corresponds to the plug flow enrichment of concentration and the liquid circulation area appears a vortex of low concentration. Thus the map of the computed velocity field or flow pattern on a tray may give us an idea about the concentration distribution. By this means, improvements can be made to the tray design, for instance, changing the construction of the inlet weir to reduce the liquid circulation in order to achieve higher enhancement of concentration across the tray or better tray efficiency.

6 CONCLUSIONS

A pseudo-single fluid computational fluid-dynamics (CFD) model for describing the liquid phase flow on a column tray is presented. Experimental measurement of local liquid velocity was conducted in an air-water simulator of 1.2 m in diameter for verifying the present model. The model predictions are confirmed by the authors' measurement and the data available from the literature, both having high percentage of liquid phase circulation area on the tray. By solving simultaneously the CFD and mass transfer equations, the concentration field on a tray can be obtained for the purpose of providing a sound basis to evaluate the enhancement of liquid phase concentration across a tray, which is very important in the design of large diameter column.

NOMENCLATURE

A	bubbling area of a tray, m^2
C_1, C_2, C_3, C_μ	turbulent model constants
C_r	coefficient of momentum transfer
c	concentration, $kg\cdot mol\cdot m^{-3}$
D	diameter of the tray, m
D_e	effective diffusivity, $m^2\cdot s^{-1}$
E_{MV}	Murphree tray efficiency
E_{OG}	Murphree point efficiency
F_0	gas (vapor) flow factor ($F_0 = w\sqrt{\rho_v}$), $kg^{1/2}\cdot m^{-1/2}\cdot s^{-1}$
f_x	body force in x direction, N
f_y	body force in y direction, N
G_p	generation of turbulent energy by bubbling and frictional Resistance, $m^2\cdot s^{-3}$
G_T	generation of turbulent energy by fluid flow, $m^2\cdot s^{-3}$
h	height of clear liquid, m
h_w	outlet weir height, mm
J	rate of mass transfer, $kg\cdot mol^{-1}\cdot m^{-2}\cdot s^{-1}$
$k_g a$	vapor phase mass transfer coefficient, $kg\cdot mol^{-1}\cdot m^{-3}\cdot s^{-1}$
$k_l a$	liquid phase mass transfer coefficient, $kg\cdot mol^{-1}\cdot m^{-2}\cdot s^{-1}$
k	turbulent kinetic energy, N·m
L	intensity of liquid flow, $m^2\cdot s^{-1}$
l_w	length of outlet weir, m
M_{Tx}	momentum loss of liquid in x direction, $kg\cdot m\cdot s^{-1}$
M_{Ty}	momentum loss of liquid in y direction, $kg\cdot m\cdot s^{-1}$
m	equilibrium constant, $m = \dot{y}/\dot{x}$
n_T	total number of grids
n_w	number of grids at the outlet weir
p	pressure, Pa
T	percentage of circulating flow area to the effective tray area, %
u	local velocity in x-direction, $m\cdot s^{-1}$
V	total volume of vapor flow, $m^3\cdot s^{-1}$
v	local velocity in y-direction, $m\cdot s^{-1}$
W	length of outlet of weir, m
w	superficial gas (vapor) velocity, $m\cdot s^{-1}$
X	dimensionless concentration
X_w	dimensionless concentration at the exit weir
x	coordinate in x direction
$\dot{x}$	mole fraction of a component in liquid phase
$\dot{x}^*$	$\dot{x}$ in equilibrium with $\dot{y}$
$\dot{x}_{in}$	$\dot{x}$ at inlet weir
y	coordinate in y direction
$\dot{y}$	mole fraction of a component in vapor phase
$\dot{y}^*$	$\dot{y}$ in equilibrium with $\dot{x}$
α_l	mass fraction of liquid in liquid phase
α_b	mass fraction of bubble (vapor) in liquid phase
ε	dissipation rate of turbulent kinetic energy, $N\cdot s^{-1}$
η	enrichment ratio
ϑ_e	effective viscosity, $m^2\cdot s^{-1}$
ϑ_t	turbulent viscosity, $m^2\cdot s^{-1}$
μ	viscosity of the fluid, $kg\cdot s^{-1}\cdot m^{-1}$
ρ	density of the fluid, $kg\cdot m^{-3}$
ρ_l	density of liquid, $kg\cdot m^{-3}$
ρ_b	density of bubble (vapor), $kg\cdot m^{-3}$
τ_w	stress tensor near the wall, $kg\cdot m\cdot s^{-2}$
σ_k, σ_ε	turbulent model constants

REFERENCES

1 Yoshida, H., "Liquid flow over distillation column tray", *Chem. Eng. Comm.*, **51**, 261—275 (1987).
2 Zhang, M.Q., Yu, K.T., "Simulation of two dimensional liquid qhase flow on a distillation tray", *Chinese J. Chem. Eng.*, **2** (2), 63—71 (1994).
3 Yu, K.T., Yuan, X.G., You, X.Y., Liu, C.J., "Computational fluid-dynamics and experimental verification of two-phase two-dimensional flow on a sieve column tray", *Chem. Eng,. Res. Des.*, **77**(Part A) 554—560 (1999).
4 Porter, K.E., Yu, K.T., Chambers, S., Zhang, M.Q., "Flow patterns and temperature profiles on a 2.4 m diameter sieve tray", *IChemE Symp. Series No. 128, Distillation and Absorption*, A257—A273 (1992).
5 Krishna, R., van Baten, J.M., Ellenberger, J., Higler, A.P., Taylor, R., "CFD simulations of sieve tray hydrodynamics", *Chem. Eng,. Res. Des.*, **77**(Part A), 639 (1999).
6 Nallasamy, M., "Turbulent models and their applications to the prediction of internal flows: A review", *Computer and Fluids*, **15** (2), 151—171 (1987).
7 Patankar, S.V., Numerical Heat Transfer and Fluid Flow, Hemisphere Publishing Corporation and MacGraw Hill Book Company, New York (1980).
8 Launder, B.E., Spalding, D.E., Comp. "The numerical computation of turbulent flows", *Meth. Appl. Mech. Eng.*, **23**, 269—279 (1974).
9 Bennett, C.O., Meyers, J.E., Momentum, Heat and Mass Transfer, MacGraw Hill Book Company, New York (1982).
10 American Institute of Chemical Engineers, Bubble-Tray Design Manual, AIChE, New York (1958).
11 Yu, K.T., Huang, J., Li, J.L., Song, H.H., "Two dimensional flow and eddy diffusion on a sieve tray", *Chem. Eng. Sci.*, **45** (9), 2901—2906 (1990).